Supporting Information

New honeycomb metal-carboxylate-tetrazolate framework with multiple functions in CO_2 conversion and selective capture for C_2H_2, CO_2 and benzene

Gang-Ding Wang,[a] Yong-Zhi Li,[a] Wen-Juan Shi,[a] Lei Hou,*[a] Zhonghua Zhu,[b] and Yao-Yu Wang[a]

[a]Key Laboratory of Synthetic and Natural Functional Molecule Chemistry of the Ministry of Education, National Demonstration Center for Experimental Chemistry Education (Northwest University), College of Chemistry & Materials Science, Northwest University. Xi'an, 710069, P. R. China. E-mail: lhou2009@nwu.edu.cn;

[b]School of Chemical Engineering, The University of Queensland, Brisbane 4072, Australia

*To whom correspondence should be addressed. E-mail: lhou2009@nwu.edu.cn (Lei Hou).

Contents

1. IR spectrum, TGA and Pore size distribution

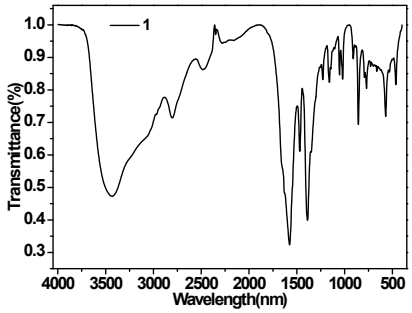

Fig. S1 FTIR spectra of the as-synthesized **1**.

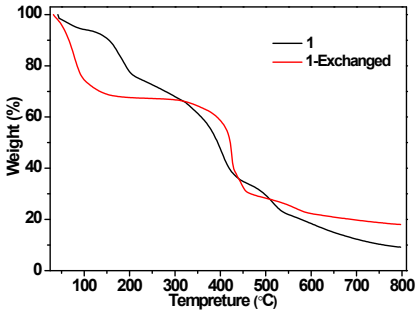

Fig. S2 TGA curves of as-synthesized and exchanged samples of **1**.

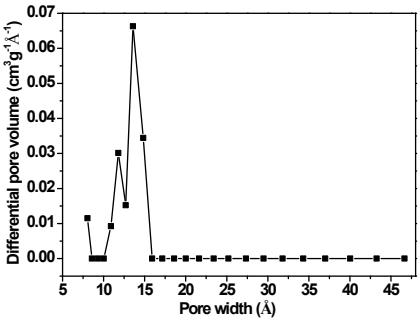

Fig. S3 Porous distribution curve calculated from N_2 adsorption isotherm using the Horvath-Kawazoe model.

2. Calculation of sorption heat

$$\ln P = \ln N + 1/T\sum_{i=0}^{m} a_i N^i + \sum_{i=0}^{n} b_i N^i \qquad\qquad Q_{\mathrm{st}} = -R\sum_{i=0}^{m} a_i N^i$$

The virial 2 expression was used to fit the combined isotherm data for **1a** at 273.15, 298 and 308 K, where P is the pressure, N is the adsorbed amount, T is the temperature, a_i and b_i are virial coefficients, and m and N are the number of coefficients used to describe the isotherms. Q_{st} is the coverage-dependent enthalpy of adsorption and R is the universal gas constant.

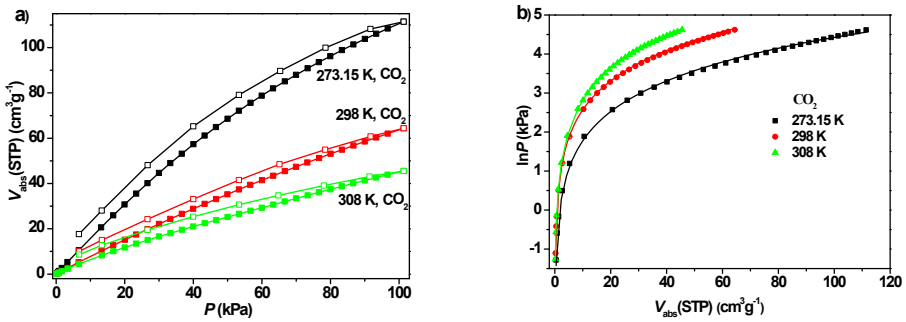

Fig. S4 a) adsorption isotherms of **1a** for CO_2 at 273.15, 298 and 308 K; b) fitted CO_2 adsorption isotherms, fitting results: a0 = -2611.34546, a1 =1.53137, a2 = -0.00439, b0 = 8.98102, Chi^2 = 0.00414, R^2 = 0.99835.

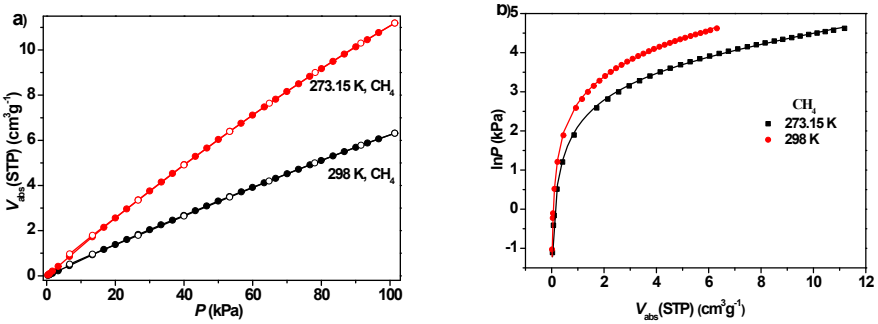

Fig. S5 a) adsorption isotherms of **1a** for CH_4 at 273.15 and 298 K (Due to the adsorption amount of CH_4 at 308 K is too low, the adsorption isotherms at 273.15 and 298 K were used for adsorption heat calculation); b) fitted CH_4 adsorption isotherms, fitting results: a0 = -2092.71309, a1 = -6.73453, a2 = 0.84735, b0 = 9.7922, Chi^2 = 0.00311, R^2 = 0.99874.

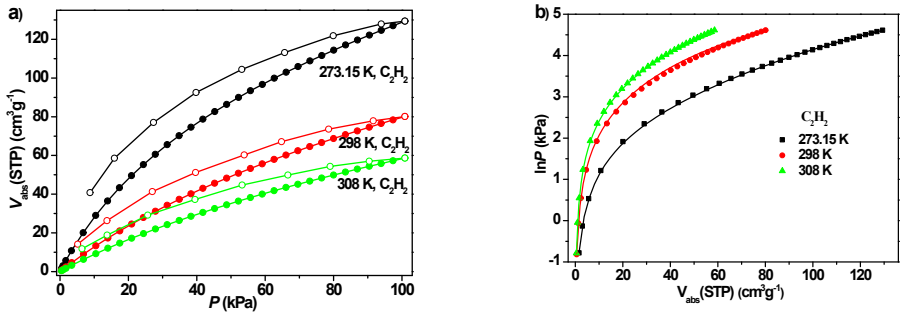

Fig. S6 a) adsorption isotherms of **1a** for C_2H_2 at 273.15, 298 and 308 K; b) fitted C_2H_2 adsorption isotherms, fitting results: a0 = -3002.82058, a1 = -15.34841, a2 = 0.23517, a3 = -0.00007, b0 = 9.74003, b1 =0.06155, b2 = -0.00081, Chi^2 = 0.00121, R^2 = 0.99941.

3. Selectivity prediction

The experimental isotherm data for pure gas A, and gas B were fitted at 298 K using a dual Langmuir-Freundlich (L-F) model (Fig. S7):

$$q = \frac{a_1 * b_1 * P^{c_1}}{1 + b_1 * P^{c_1}} + \frac{a_2 * b_2 * P^{c_2}}{1 + b_2 * P^{c_2}}$$

Where q and p are adsorbed amounts and the pressure of component i, respectively.

The adsorption selectivities for binary mixtures of gas A and gas B, defined by

$$S_{i/j} = \frac{x_i * y_j}{x_j / y_i}$$

were respectively calculated using the Ideal Adsorption Solution Theory (IAST) of Myers and Prausnitz. Where xi is the mole fraction of component i in the adsorbed phase and yi is the mole fraction of component i in the bulk.

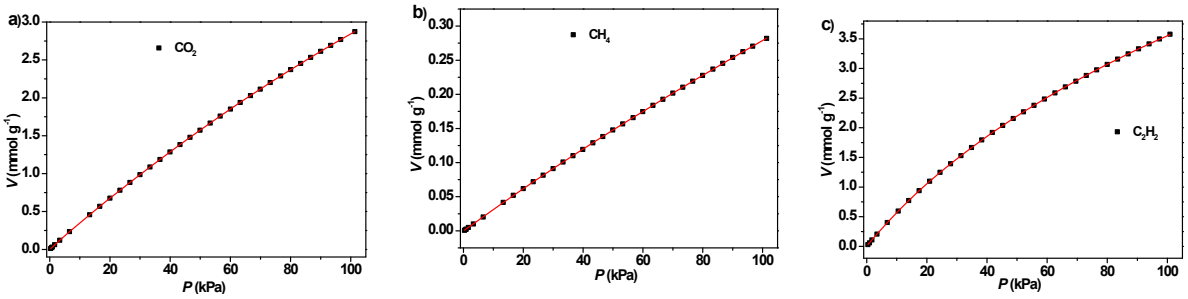

Fig. S7 a) Fitted CO_2 adsorption isotherm: a1 = 10.87605, b1 = 0.00197, c1 = 1.11169, a2 = 0.16549, b2 = 0.09675, c2 = 0.98184, Chi^2 = 4.0333E-7, R^2 = 1; b) fitted CH_4 adsorption isotherm: a1 = 2.8941, b1 = 0.00099, c1 = 1.01107, a2 = 0.00704, b2 = 0.01641, c2 = 1.4379, Chi^2 = 5.8543E-8, R^2 = 0.99999; c) fitted C_2H_2 adsorption isotherm: a1 = 10.83758, b1 = 0.00606, c1 = 0.94884, a2 = 0.04347, b2 = 0.00091, c2 = 2.78385, Chi^2 = 4.9104E-6, R^2 =1.

4. Mechanism for the catalytic reaction

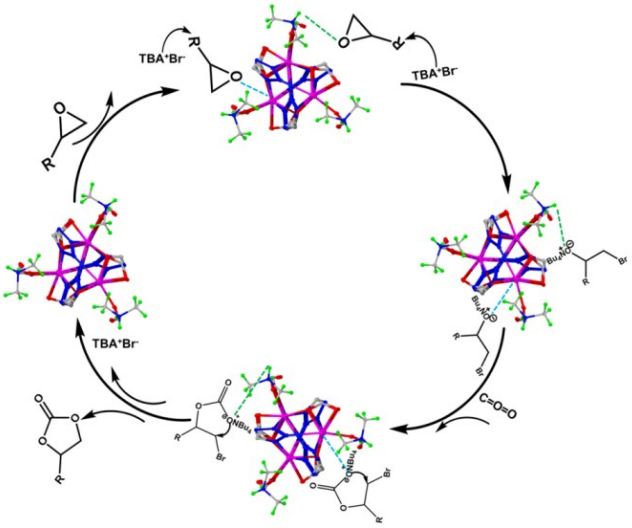

Fig. S8 Mechanism for the catalytic conversion of CO_2 with epoxides.

5. Fitted adsorption isotherms of Bz and Cy

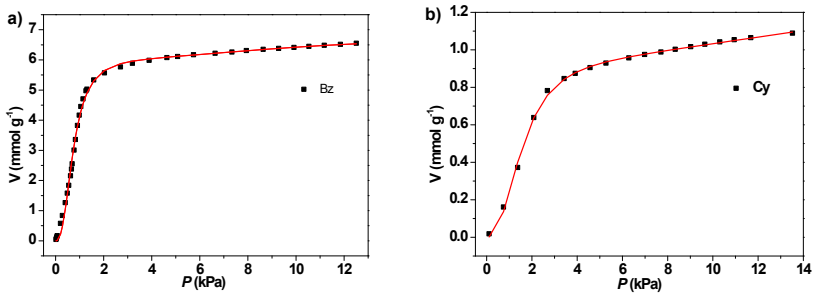

Fig. S9 a) Bz adsorption isotherm of **1a** fitted by dual L-F model: 298 K, a1 = 6.08651, b1 = 2.08767, c1 = 2.54133, a2 = 0.65089, b2 = 0.0009, c2 = 3.09494, Chi^2 = 0.02019, R^2 = 0.99673; (b) Cy adsorption isotherm of **1a** fitted by L-F model: 298 K, a1 = 0.97135, b1 = 0.33051, c1 = 2.38574, a2 = 0.38835, b2 = 0.00067, c2 = 2.53741, Chi^2 = 0.00019, R^2 = 0.99857.

6. GCMC simulation methodlody

Grand canonical Monte Carlo (GCMC) simulations were performed for the gas adsorption in the framework by the Sorption module of Material Studio (Accelrys. Materials Studio Getting Started, release 5.0). The framework was considered to be rigid, and the optimized gas and epoxide molecules were used. The partial charges for atoms of the framework were derived

from QEq method and QEq_neutral 1.0 parameter. One unit cell was used during the simulations. The interaction energies between the gas molecules and framework were computed through the Coulomb and Lennard-Jones 6-12 (LJ) potentials. All parameters for the atoms were modeled with the universal force field (UFF) embedded in the MS modeling package. A cutoff distance of 12.5 Å was used for LJ interactions, and the Coulombic interactions were calculated by using Ewald summation. For each run, the 3×10^6 maximum loading steps, 3×10^6 production steps were employed.

7. Table of crystallographic data

Table S1. Crystallographic data for **1**.

Chemical formula	$C_8H_{10}CdN_5O_4$
Formula weight	352.62
T (K)	296(2)
Crystal system	Trigonal
Space group	R-3
a (Å)	32.068(3)
b (Å)	32.068(3)
c (Å)	8.244(1)
α, β, γ(°)	90, 90, 120
V (Å^3)	7342.0(19)
Z	18
$D_{calcd.}$(g·cm^{-3})	1.436
μ (mm^{-1})	1.350
Reflns collected, unique, R_{int}	2991, 2991, 0.0626
Goof	1.182
R_1[a], wR_2[b] (I > 2σ)	0.0883, 0.2380
R_1[a], wR_2[b] (all data)	0.0885, 0.2382

[a] $R_1 = \Sigma||F_o| - |F_c||/\Sigma|F_o|$; [b] $wR_2 = [\Sigma w(F_o^2 - F_c^2)^2/\Sigma w(F_o^2)^2]^{1/2}$.

Table S2. Selected bond lengths [Å] and angles [°] for **1**.

Cd(1)-O(3)	2.266(13)	N(1)-Cd(1)-N(3)#1	152.3(4)	O(1)-Cd(1)-O(1)#2	142.0(3)
Cd(1)-N(1)	2.272(10)	O(3)-Cd(1)-O(1)	85.2(5)	O(3)-Cd(1)-O(2)#2	80.3(5)
Cd(1)-N(3)#1	2.299(10)	N(1)-Cd(1)-O(1)	83.7(4)	N(1)-Cd(1)-O(2)#2	100.6(5)
Cd(1)-O(1)	2.353(10)	N(3)#1-Cd(1)-O(1)	79.3(4)	N(3)#1-Cd(1)-O(2)#2	101.4(6)
Cd(1)-O(1)#2	2.428(10)	O(3)-Cd(1)-O(1)#2	132.1(5)	O(1)-Cd(1)-O(2)#2	165.5(4)

O(3)-Cd(1)-N(1)	110.5(6)	N(1)-Cd(1)-O(1)#2	88.0(3)	O(1)#2-Cd(1)-O(2)#2	52.4(4)
O(3)-Cd(1)-N(3)#1	89.7(6)	N(3)#1-Cd(1)-O(1)#2	92.1(4)		

Symmetry codes: #1 = 1/3-x+y, 2/3-x, z+2/3, #2 = 1/3-x+y, 2/3-x, z-1/3, #3 = 2/3-y, x-y+1/3, z+1/3, #4 = 2/3-y, x-y+1/3, z-2/3, #5 = 1/3-x, 2/3-y, 2/3-z.

8. Comparison of adsorption data of Bz and Cy

Table S3. Benzene and cyclohexane adsorption amounts and selectivity for **1** compared with various reported porous materials at 298 K.

Material	Bz (cm^3g^{-1})	Cy (cm^3g^{-1})	Selectivity	Reference
COF-1	220.0	87.0		1
Mn-MOF-74	210.1	5.6	--	2
Co-MOF-74	124.8	5.2	10^5	
Zn-MOF-74	151.1	3.8	--	
1	146.7	24.4	7086	This work
MFOF-1	90.5	34.3	--	3
Ce-LOF	89.0	41.4	13.6	4
$Ni_3(OH)(Ina)_3(BDC)_{1.5}$	84.1	3.8	--	5
MAF-2	59.2	--	--	6
$\{[Cd(ATAIA)]\cdot 4H_2O\}_n$	52	8		7
PCN-TPC	50.5	19.7	--	8
PAF-2	39.6	2.3	--	9
DAT-MOF-1	33.6	4.5	200	10
2-bpe	31.0	2.7	--	11

References

[1] P. Dasa and S. K. Mandal, A dual-functionalized, luminescent and highly crystalline covalent organic framework: molecular decoding strategies for VOCs and ultrafast TNP sensing, *J. Mater. Chem. A*, 2018, **6**, 16246-16256.

[2] S. Mukherjee, B. Manna A. V. Desai, Y. Yin, R. Krishna, R. Babarao and S. K. Ghosh, Harnessing Lewis acidic open metal sites of metal-organic frameworks: the foremost route to achieve highly selective benzene sorption over cyclohexane, *Chem. Commun.,* 2016, **52**, 8215-8218.

[3] L. Zhang, W. Yang, X. -Y. Wu, C. Z. Lu and W. Z. Chen, A Hydrophobic Metal–Organic Framework Based on Cubane-Type $[Co_4(\mu_3\text{-}F)_3(\mu_3\text{-}SO_4)]^{3+}$ Clusters for Gas Storage and Adsorption Selectivity of Benzene over Cyclohexane, *Chem. Eur. J*, 2016, **22**, 11283-11290.

[4] Z. Lin, R. Zou, W. Xia, L. Chen, X. Wang, F. Liao, Y. Wang, J. Lin and A. K. Burrell, Ultrasensitive sorption behavior of isostructural lanthanide-organic frameworks induced by lanthanide contraction, *J. Mater. Chem*., 2012, **22**, 21076-21084.

[5] G. Ren, S. Liu, F. Ma, F. Wei, Q. Tang, Y. Yang, D. Liang, S. Li and Y. Chen, A 9-

connected Metal-Organic Framework with Gas Adsorption Properties. *J. Mater. Chem*., 2011, 21, 15909-15913.

[6] J.-P. Zhang and X. M. Chen, Exceptional Framework Flexibility and Sorption Behavior of a Multifunctional Porous Cuprous Triazolate Framework, *J. Am. Chem. Soc*., 2008, **130**, 6010-6017.

[7] P. Das and S. K. Mandal, Strategic Design and Functionalization of an Amine-decorated Luminescent Metal Organic Framework for Selective Gas/Vapor Sorption and Nanomolar Sensing of 2,4,6-Trinitrophenol in Water, *ACS Appl. Mater. Interfaces*., 2018, **10**, 25360-25371.

[8] G. Deng and Z. Wang, Triptycene-Based Microporous Cyanate Resins for Adsorption/Separations of Benzene/Cyclohexane and Carbon Dioxide Gas, *ACS Appl. Mater. Interfaces*, 2017, **9**, 41618-41627.

[9] H. Ren, T. Ben, E. Wang, X. Jing, M. Xue, B. Liu, Y. Cui, S. Qiu and G. Zhu, Targeted synthesis of a 3D porous aromatic framework for selective sorption of benzene, *Chem. Commun.,* 2010, **46**, 291-293.

[10] B. Manna, S. Mukherjee, A. V. Desai, S. Sharma, R. Krishna and S. K. Ghosh, A π-electron deficient diaminotriazine functionalized MOF for selective sorption of benzene over cyclohexane, *Chem. Commun*., 2015, **51**, 15386-15389.

[11] C. X. Ren, L. X. Cai, C. Chen, B. Tan, Y. J. Zhang and J. Zhang, π-Conjugation-directed highly selective adsorption of benzene over cyclohexane, *J. Mater. Chem. A*, 2014, **2**, 9015-9019.

9. ^{1}H NMR spectra characterization

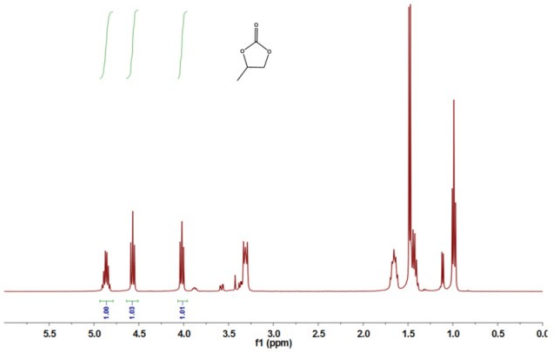

^{1}H NMR spectrum of propylene carbonate in $CDCl_3$.

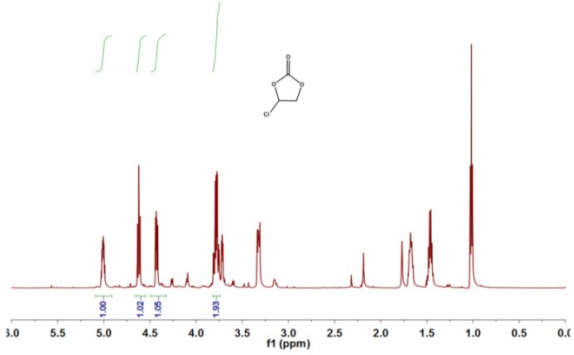

^{1}H NMR spectrum of 4-cloromethyl-1, 3-dioxolan-2-one in $CDCl_3$.

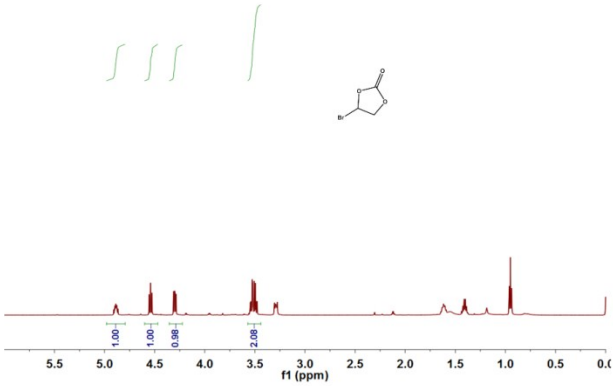

^{1}H NMR spectrum of 4-bromomethyl -1, 3-dioxolan-2-one in $CDCl_3$.

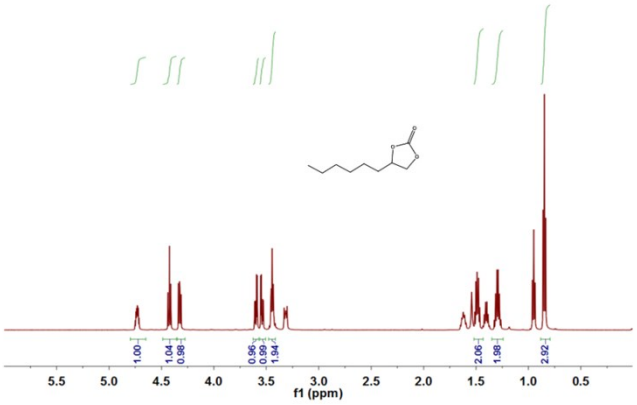

^{1}H NMR spectrum of 3-butoxy-1, 2-propylene carbonate in $CDCl_3$.

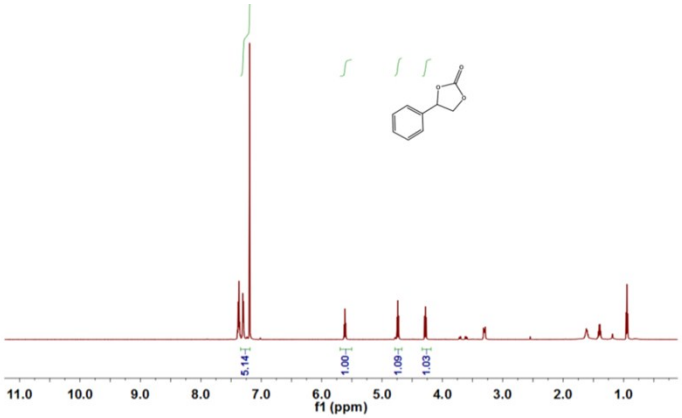

H NMR spectrum of styrene carbonate in $CDCl_3$.